Match Elimination using Cycle Basis in Underwater Optical Mapping

Armagan Elibol and Jinwhan Kim
Division of Ocean Systems Engineering
KAIST, Daejeon, Korea
{aelibol,jinwhan}@kaist.ac.kr

Son-Cheol Yu
Dept. of Creative IT Excellence Eng.
POSTECH, Pohang, Korea
sncyu@postech.ac.kr

Nuno Gracias and Rafael Garcia
Computer Vision and Robotics Group
University of Girona, Girona, Spain
ngracias@eia.udg.edu,rafael.garcia@udg.edu

***Abstract*—The use of image mosaicing methods for underwater optical mapping has become very popular owing to the rapid progress in obtaining optical data using robotic platforms. In order to obtain globally consistent mosaics, one of the essential steps is global alignment for finding best image registration parameters, which employs non-linear optimisation methods to minimise the error metric defined over correspondences detected between overlapping image pairs. In this paper, we propose a method that uses graph theory principles to reduce the total number of overlapping image pairs used in the global alignment process without degrading the final mosaic quality. This reduction allows for obtaining image mosaics with reduced computational cost and time. The method is validated through two experiments that involve challenging underwater datasets.**

I. INTRODUCTION

Although the oceans cover 70% of the surface of Earth, our knowledge and understanding of processes happening there has been very limited for a long time due to the lack of imaging techniques. Over the last two decades, notable progress in developing underwater robotic platforms has been achieved. These achievements nowadays allow for obtaining optical information, which is a rich source of information for scientists working in various underwater research fields (*e.g.*, geology [1], ecology [2] and archeology [3]).

Visual sensors provide much more detailed information than acoustic sensors and have become less expensive, smaller and lighter. As a result, their usage has increased considerably even in commercially available small underwater platforms [4], [5]. However, optical imaging in underwater environments has to overcome several additional difficulties due to poor visibility, light absorption, forward and back scattering, and non-uniform illumination. These challenges force images to be acquired in close range to the seabed. As a consequence, the area of interest cannot be captured in a single image. Hence, in order to have an overview of the area of interest, image mosaicing (stitching) methods [6] have become a requisite. Image mosaicing is a process of combining several relatively smaller images to make one larger image, known as mosaic and/or photo-mosaic. Image mosaicing has been extensively studied and widely used in both computer vision and robotics communities mainly for visual mapping purpose in aerial [7] and underwater environments [8]. Most of the existing image mosaicing approaches assume that time-consecutive images can be properly registered [9]. Under this assumption, the relative displacement among pairs of images can be obtained by cascading the motion parameters that relate time-consecutive images [10]. However, in the absence of absolute orientation and/or position information, the cascading of time-consecutive motion estimates results in error growth, typical of dead-reckoning positioning [10]. If the trajectory of a camera revisits an area that has been imaged before, the trajectory provides a loop closure, and it is called closed-loop trajectory. This type of trajectories provide an overlapping area between non time-consecutive images, which are essential to minimise the dead-reckoning error by the use of global alignment methods. Therefore, it is very important to identify overlapping image pairs to get a globally coherent mosaics.

Global alignment can be defined as the problem of finding the image-to-mosaic registration parameters that best comply with constraints introduced by all overlapping image pairs. Global alignment requires the minimisation of an error term, which is defined on the positions of image correspondences. Commonly, this minimisation employs nonlinear methods, which incurs high computational cost [11] due to its iterative structure. This computational cost is considerably high especially for large area surveys, which may contain from several hundreds to thousands of images.

Several image mosaicing approaches have been presented over the last two decades [6], [12], [13]. Sawhney et. al. [12] proposed a complete solution for image mosaicing where the topology (the trajectory of the camera and overlapping image pairs) is iteratively estimated. Spatial consistency is improved by identifying and registering non-time consecutive images. They used the graph representation to denote the topology where nodes are images and edges represent that there is an overlapping area between nodes. They constructed the graph taking into account image positions with respect to the chosen global frame. This requires an initial position estimation of the images which is obtained through the assumption that time-consecutive images have an overlap. The initial estimate is obtained by accumulating pairwise homographies. Potential overlapping image pairs are generated and added by computing a normalised distance on image positions and comparing to their alternative path distance. This method performs well for image sequences that are composed of relatively few images and/or whose camera motion is very small and the initial estimation is more likely to suffer less from error accumulation. However it is not feasible for mapping large area environments where time-consecutive images might not have an overlap and/or suffering drastically trajectory drift. In terms of edge quality in the graph, Ila *et al.* [14] proposed a method to keep the most informative edges between robot

978-1-4799-0002-2/13/$31.00 ©2013 IEEE

poses using Mutual Information (MI) within a Simultaneous Localisation and Mapping (SLAM) context to maintain the sparsity of the system. However, our problem considered in this paper is to select a subset of overlapping image pairs to be used in the global alignment process for a given all overlapping image pairs, which is a different problem to that of performing matches and keeping some of them from the most recent image to all previous images as the robot moves.

Some recent studies have used image-to-mosaic registration [15], [16] with the aim of real time mosaicing (known as "online mosaicing") to discard some images and to select key frames [17], [18]. These approaches are mainly targeted for creating panoramic mosaics from a video sequence, where images have large overlapping areas, especially the cases where the camera only rotates. In the case of online mosaicing, if mapping one image onto the mosaic fails then the following future image-to-mosaic registrations will most likely fail. On the other hand in visual mapping with robotic platforms, large overlapping areas between images cannot be assumed. Moreover, large area surveys (usually taking several days to complete) tend to have minimal overlap among images due to the energy management of the acquisition platform.

In this paper, we discuss the importance of overlapping pairs and propose a method based on a graph theory to reduce the total number of overlapping image pairs used in the global alignment process without compromising the final registration quality of the mosaic, thus providing a huge saving on the computational cost. We assume that all the overlapping image pairs have been identified a priori. We present initial results on real underwater images acquired by an underwater robot.

The remainder of the paper is organised as follows: section II gives a brief summary about Feature-based Image Mosaicing (FIM). Next, section III is devoted to detail the proposed method to reduce the overlapping image pairs to be used in the global alignment process. Some exploratory results are illustrated in section IV and, finally, we present our conclusions and future works in the last section.

II. Overview of Feature-based Image Mosaicing (FIM)

FIM is based on finding consistent corresponding points between image pairs to create a mosaic image. It can be divided into two main steps: pairwise and global alignments. While pairwise alignment is used to find the registration parameters between two overlapping images, global alignment searches for registration parameters for mapping to a common frame, also known as the *global frame*, in order to have the global view of the surveyed area.

Pairwise image alignment (or registration) is the process of overlaying two views of the same scene taken from different viewpoints. Several approaches exist to register images [19]. Feature-based methods rely on the detection of distinctive points using feature detectors such as Harris [20], Hessian [21] or Laplacian [22]. These features are found in the two images to be registered, and then a cross-correlation or Sum of Squared Differences (SSD) score is computed for each feature involving geometric transformation of the image. This had been the trend for a long time until the advent of Scale Invariant Feature Transform (SIFT) algorithm [23], which has taken feature-based methods to the forefront. Compared to all previous schemes, SIFT and further developed methods such as Speeded Up Robust Features (SURF) [24] perform much better and show considerably greater invariance to image scaling, rotation, robustness under change in both illumination and 3D camera viewpoint. These methods solve the correspondence problem through a feature description and descriptor matching. After detecting features, feature descriptors exploiting gradient information at a particular orientation and spatial frequencies (see [25] for a detailed survey on descriptors) are computed. Finally, the matching of features is generally done using the Euclidean distance between their descriptors. In this way corresponding points are detected in each pair of overlapping images.

The initial matching usually provides some incorrect correspondences, which are called *outliers*. Outliers must be identified and removed, typically by the use of a robust estimation algorithm (*e.g.*, Random Sample Consensus (RANSAC) [26]). After outlier rejection, a homography can be computed from the inliers through orthogonal regression.

The goal of global alignment is to minimise a cumulative error and to build a globally coherent mosaic by aligning images correctly. Let ${}^{t-1}\mathbf{H}_t$ denote the relative homography between t^{th} and $(t-1)^{th}$ images in a sequence. If the first image of the sequence is chosen as the global frame, the global projection of image t into the mosaic frame is denoted as ${}^{1}\mathbf{H}_t$. ${}^{1}\mathbf{H}_t$ is known as the *Absolute Homography*, and it can be calculated by composing (or cascading) the relative homographies ${}^{1}\mathbf{H}_t = {}^{1}\mathbf{H}_2 \cdot {}^{2}\mathbf{H}_3 \cdot \ldots \cdot {}^{t-1}\mathbf{H}_t$. However, the detected correspondences between image pairs are subject to localisation errors, and the accuracy of the resulting homography is limited. Therefore, computing absolute homographies by cascading noisy relative homographies leads to cumulative error. Thus, global alignment reestimates the absolute homographies by best satisfying geometric constraints arising from the matches between overlapping image pairs. These matches result from consecutive and nonconsecutive (closed loop) image pairs and form an over-constrained set of equations. Global alignment is usually done by minimising the error metric defined over correspondences between image pairs. One of the well-established and widely-used methods is Bundle Adjustment (BA) [27], which minimises the following cost function below:

$$\begin{aligned}\varepsilon = \sum_k \sum_t \sum_{j=1}^{n} &\parallel {}^{k}\mathbf{x}_j - {}^{1}\mathbf{H}_k^{-1} \cdot {}^{1}\mathbf{H}_t \cdot {}^{t}\mathbf{x}_j \parallel_2 + \\ &\parallel {}^{t}\mathbf{x}_j - {}^{1}\mathbf{H}_t^{-1} \cdot {}^{1}\mathbf{H}_k \cdot {}^{k}\mathbf{x}_j \parallel_2\end{aligned} \tag{1}$$

where k and t are indices to a pair of images that were matched successfully, n is the total number of correspondences between the overlapping image pairs, and $\left({}^{1}\mathbf{H}_k, {}^{1}\mathbf{H}_t\right)$ are the absolute homographies for images k and t. The minimisation of the error term in Eq. (1) requires the use of iterative nonlinear methods operating over the Jacobian matrix of the cost function. This implies a high computational cost, since the total number of overlapping image pairs and the associated total number of correspondences used during the minimisation have a direct impact on the computational cost as one additional correspondence requires the addition of 4 more rows to the Jacobian matrix of the cost function in Eq. (1).

III. MATCH ELIMINATION WITH CYCLE BASIS

Graph theory has been behind a large number of algorithms successfully used in various science disciplines such as biology [28], electrical engineering [29], operational research [29] and several others [30].

A graph $G = (V,E)$ consists of vertices (nodes) and the edges (links) between vertices. V is the set of vertices while $E \subset V \times V$ represents the set of edges. The total number of vertices $n = |V|$ defines the order of the graph while the total number of edges $m = |E|$ is the size of the graph [31]. A graph can be classified as either directed or undirected depending on whether the edges are ordered pairs or not. A cycle in a graph is defined as a subgraph in which every vertex has even degree[1]. A cycle basis is a list of cycles in the graph, with each cycle expressed as a list of vertices [32]. These cycles form a basis for the cycle space of the graph, so that every other cycle in the graph can be obtained from the cycle basis using only symmetric differences. Commonly used methods to compute cycle basis are based on spanning trees. The spanning tree of a connected graph is a tree that connects all the nodes together [31]. One graph can have several different spanning trees. The Minimum Spanning Tree (MST) is a spanning tree whose edges have a total weight less than or equal to the total weight of every other spanning tree of the graph. The cycle basis obtained by using the MST is called the minimum weight spanning tree basis, which is computed through adding an edge to the MST and removing the path connecting the endpoints of the edge. The total number of cycles in the basis for a connected graph is

$$t_c = \left(\mathrm{m} - (\mathrm{n} - 1)\right).$$

If the graph is not connected[2] then total number of cycles in the basis is computed as

$$\left(m - (n-1) + (p-1)\right),$$

where p is the number of connected components. Every cycle that is not in the basis can be written as a linear combination of two or more cycles in the basis.

We have modelled the topology as a graph where images are vertices and successfully matched image pair represents an edge between nodes in the graph. As there will only be one edge between a pair of nodes, the graph is called a simple graph. Cycles in this graph represent closed loops among images. If homographies representing edges are multiplied sequentially, one should expect to get identity mapping inside a closed loop (*e.g.*, Fig. 1). In practice, this becomes impossible due to the error accumulation.

To compute the cycle basis through MST, weights must be assigned to edges. From existing studies [14], [33], using Observation Mutual Information (OMI) as weights is shown to be effective and provides useful information about image pairs. OMI provides how much the uncertainty of the parameters will reduce when the observation is realized. Therefore, OMI [34]

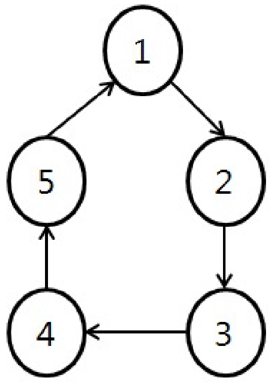

Fig. 1. Illustrative example of a cycle showing a closed-loop, which following equality is expected to be hold. $\mathbf{I} = {}^{1}\mathbf{H}_2 \cdot {}^{2}\mathbf{H}_3 \cdot {}^{3}\mathbf{H}_4 \cdot {}^{4}\mathbf{H}_5 \cdot {}^{5}\mathbf{H}_1$. However, this equality does not hold due to error accumulation. The longer it gets, the more error accumulates.

can be easily calculated from the information matrices as the change in information as follows:

$$I(k, \mathbf{z}(k)) = \frac{1}{2} \ln \left[\frac{|\mathbf{Y}(k \mid k)|}{|\mathbf{Y}(k \mid k-1)|} \right] \tag{2}$$

where the *Fisher Information* matrix $\mathbf{Y}$ [35] is the inverse of the covariance matrix of the parameters and $\mathbf{z}(k)$ is the observation value. The notation $(\cdot)(k \mid t)$ refers to a value at k given t (Further details can be seen in [33]). To compute the OMI of an image pair, trajectory estimate and its uncertainty are required [33]. Therefore, our proposal starts with an initial step where the initial trajectory is estimated and its uncertainty is propagated [33]. To have the initial estimate, each image requires at least one edge that allows it to connect to other images. This can be achieved by computing a spanning tree. If the edges are weighted, then the MST can be computed to establish the initial link between images. For each overlapping image pair, the amount of overlap between images is computed and used as a weight to compute the initial MST. While computing the MST weights are inverted so that the resulting edges in the MST are the ones that maximise the total amount of overlap between images. With using the edges in the initial MST, we estimate the initial trajectory by minimising the reprojection error given in Eq. 1 and its uncertainty is propagated by using the first order approximation [33]. After having the initial trajectory estimate and its uncertainty, the OMI of every edge in the graph is computed. The OMI values are used as weights to obtain the (weighted) cycle basis based on the newly computed MST with OMI values including the most informative image pairs. Then for every cycle c in the basis, the method checks whether all images that are in cycle c have appeared in another cycle in the basis. If so, we keep the longer cycle in the basis and remove the short one. The longer the loop, the larger error accumulates. Therefore, we keep the longer cycles, which encode more cumulative errors, and allow reducing them in the global alignment process. The overview of our proposal is illustrated in Fig. 2.

IV. EXPERIMENTAL RESULTS

Our proposal has been tested over two real datasets. The first dataset was obtained from a tank experiment using a

[1]The degree of a vertex is defined as the total number of edges incident to the vertex.

[2]In an undirected graph G, two vertices u and v are called connected if G contains a path from u to v. A graph is said to be connected if every pair of vertices in the graph is connected.

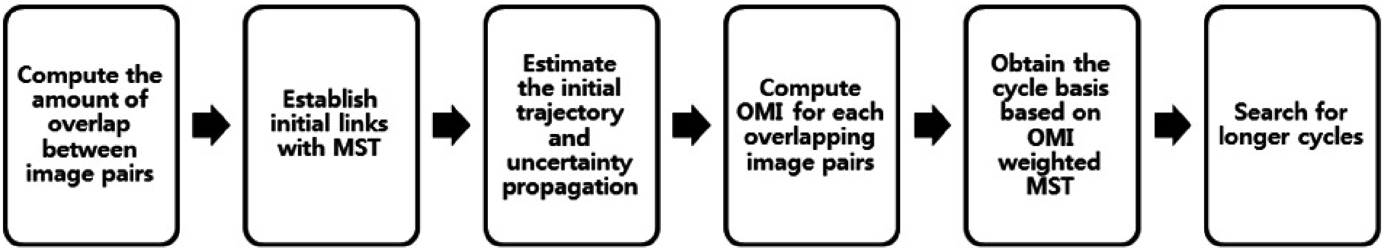

Fig. 2. Pipeline of the proposed framework.

custom-built, hover-capable Autonomous Underwater Vehicle (AUV). The vehicle was equipped with a down-looking camera and it was controlled to navigate keeping constant altitude, with the optical axis of the camera being orthogonal to the floor of the tank during the experiment to relieve any 3D effects. The dataset has 149 images of 3648×2736 resolution and the total number of successfully registered overlapping image pairs is 4621. The second dataset is composed of 2751 images. A total number of 486 key frames providing approximately 70% of overlap between time-consecutive images were selected out of the complete set. The dataset was acquired with using a Phantom XTL Remotely Operated Vehicle (ROV) operating at a distance of 2.5m from the seabed during a survey of a patch reef located in the Florida Reef Tract (depth 7-10m) near Key Largo in the U.S. [2]. Images have 512×384 resolution. The total number of successfully registered overlapping image pairs is 3225. We model the image-to-mosaic motions using similarity homographies [26] since they have enough Degrees of Freedom (DOFs) to model the trajectory of the camera under constant altitude and perpendicular optical axis to the scene. The motion has four DOFs (1-D rotation (θ), 2-D translation (t_x and t_y), and 1-D scaling (s)) and it has the following form:

$$H = \begin{bmatrix} s \cdot \cos(\theta) & -s \cdot \sin(\theta) & t_x \\ s \cdot \sin(\theta) & s \cdot \cos(\theta) & t_y \\ 0 & 0 & 1 \end{bmatrix}$$

Since our problem is batch mosaicing, it can be assumed that all images are available at the beginning of the process and can be registered using image registration algorithms (*e.g.*, using SIFT [23]). For global alignment, we used BA [27], which minimises the error given in Eq. 1. The error was minimised using large-scale nonlinear least squares methods. We have derived analytic expressions for computing the Jacobian matrix containing the derivatives of all residuals with respect to all trajectory parameters. The average reprojection error over all correspondences was compared since this error does not depend on the selected global frame. The reprojection error will remain the same regardless of the selected global coordinate frame. Hence, the first image frame is chosen as a global frame. Tests were performed in a server with a four Quad-Core AMD Opteron ™ 2.4 Ghz processor, 128 GB RAM and with a 64-bit operating system, running on MATLAB™ environment.

Table I summarises the results that compare the original and the elimination algorithm applied. The third column shows the total number of image pairs that were used to minimise the error metric defined on Eq. (1). The fourth column represents the average reprojection error computed over all correspondences while the fifth includes the standard deviation of the error. The last column shows the required computational time for the minimisation process measured by the *cputime()* function of MATLAB.

From the results, it can be observed that performing global alignment with the reduced number of overlapping image pairs provides similarly satisfactory trajectory accuracy as the one using all overlapping pairs, but with significant time saving. The obtained mosaics are visually quite similar, as they can be seen in Figs. 3(a) and 3(b).

V. Conclusions and Future Work

High-resolution optical maps (mosaics) of the seabed have been very important tools for marine scientists. Data collection in areas beyond human reach has been one of the main bottlenecks. This issue has been mainly resolved owing to the recent developments in robotic platforms. However, optical imaging in underwater environment does not allow a large area to be seen in a single image due to the difficulties (*e.g.*, scattering, absorption). This increases the necessity of methods to combine several images into a one common image, which is known as image mosaicing. One of the crucial steps of image mosaicing is global alignment, which refers to the process of finding optimal image-to-mosaic motion parameters for each image by taking into account the constraints imposed by correspondences. Global alignment is usually accomplished through nonlinear minimisation of an error metric defined on the positions of correspondences. Therefore, global alignment directly depends on the total number of overlapping image pairs and thus the total number of correspondences. In this paper, our work is aimed to reduce the computational resources and time needed for the global alignment process by leaving some overlapping image pairs out of this process without disturbing the resulting mosaic quality. We present a method that keeps the longer cycles in the computed cycle basis. The cycle basis is computed using OMI values as edge weights. The method does not require any heuristics for parameter tuning.

Future directions will be on computing and assigning different weights for each edge on the graph and finding different weighted cycle bases for further improvements.

Acknowledgment

This research was supported by the WCU (World Class University) program through the National Research Founda-

[3] The current form of our implementation is not optimised for speed. The reported execution times are included to provide an estimate of the time saving between the reduced and the original datasets.

TABLE I. SUMMARY OF RESULTS FOR THE TESTED DATASET.

Dataset	Strategy	Total Number of Edges	Total Number of Correspondences	Avg. Error in pixels	Std. Deviation in pixels	Time[3] in seconds
Dataset 1 (149 Images)	**With Elimination**	2,285	1,118,404	11.20	5.41	4,172
	Original	4,621	2,198,311	8.59	3.71	9,499
Dataset 2 (486 Images)	**With Elimination**	1,544	166,070	7.45	3.52	1,463
	Original	3,225	360,262	6.09	2.70	3,291

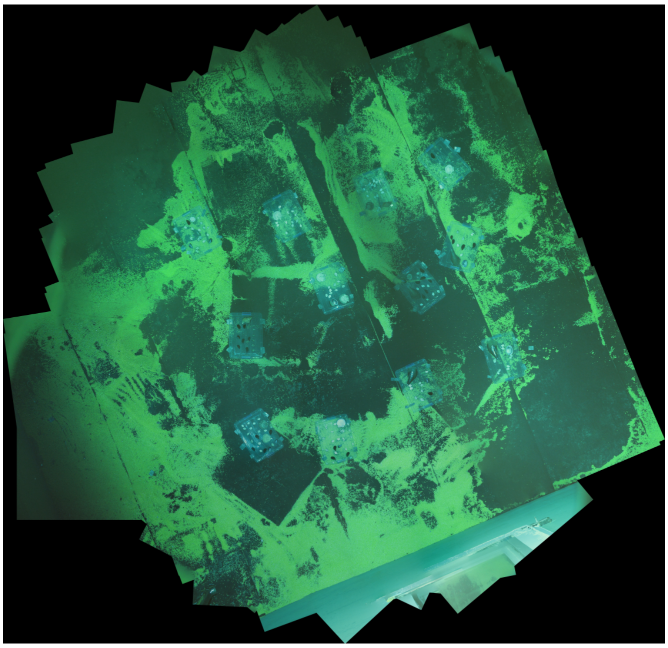

(a) Resulting mosaic obtained by using all overlapping image pairs

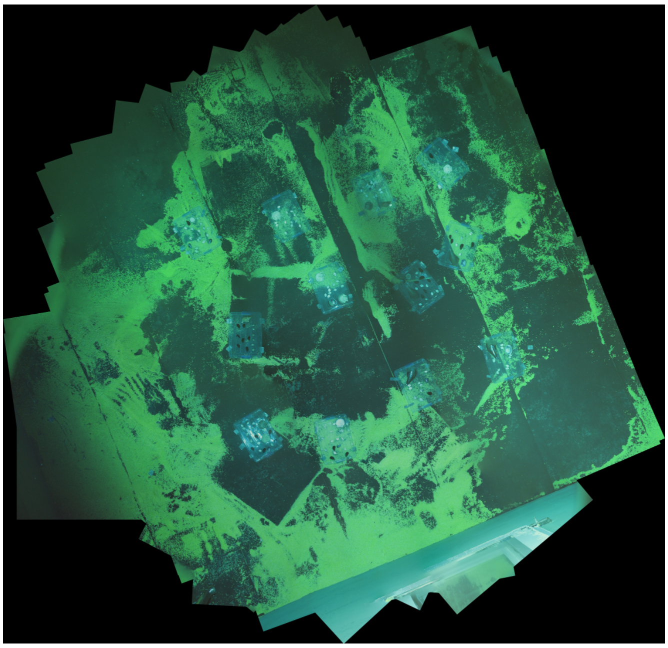

(b) Resulting mosaic obtained by using the reduced set of overlapping image pairs

Fig. 3. Final mosaics of the first dataset. Mosaics are approximately $10,000 \times 9800$ pixels and they were blended by using the method in [36].

tion of Korea funded by the Ministry of Education, Science and Technology (R31-2008-000-10045-0) and the Human Resources Development of the Korea Institute of Energy Technology Evaluation and Planning (KETEP) grant funded by the Korea government Ministry of Knowledge Economy (No. 0114030200040), and was also partially funded through EU projects FP7-ICT-2011-288704 (Morph) and FP7-INFRASTRUCTURES-312762 (EUROFLEETS2), and the Spanish Ministry of Science and Innovation (MCINN) under grant CTM2010-15216 (MuMap).

REFERENCES

[1] J. Escartin, R. Garcia, O. Delaunoy, J. Ferrer, N. Gracias, A. Elibol, X. Cufi, L. Neumann, D. J. Fornari, S. E. Humpris, and J. Renard, “Globally aligned photomosaic of the Lucky Strike hydrothermal vent field (Mid-Atlantic Ridge, 3718.5’N): Release of georeferenced data, mosaic construction, and viewing software,” *Geochemistry Geophysics Geosystems*, vol. 9, no. 12, p. Q12009, 2008.

[2] D. Lirman, N. Gracias, B. Gintert, A. Gleason, R. P. Reid, S. Negahdaripour, and P. Kramer, “Development and application of a video–mosaic survey technology to document the status of coral reef communities,” *Environmental Monitoring and Assessment*, vol. 159, pp. 59–73, 2007.

[3] B. Bingham, B. Foley, H. Singh, R. Camilli, K. Delaporta, R. Eustice, A. Mallios, D. Mindell, C. Roman, and D. Sakellariou, “Robotic tools for deep water archaeology: Surveying an ancient shipwreck with an autonomous underwater vehicle,” *Journal of Field Robotics*, vol. 27, no. 6, pp. 702–717, 2010.

[4] “GNOM Standard ROV,” Retrieved from http://www.gnom-rov.com/products/gnom-standard/, March 2013.

[5] “SeaBotix LBV150-4 MiniROV,” Retrieved from http://www.seabotix.com/products/lbv150-4.htm, March 2013.

[6] R. Szeliski, “Image alignment and stitching: A tutorial,” *Foundations and Trends® in Computer Graphics and Vision*, vol. 2, no. 1, pp. 1–104, 2006.

[7] F. Caballero, L. Merino, J. Ferruz, and A. Ollero, “Homography based Kalman filter for mosaic building. applications to UAV position estimation,” in *IEEE International Conference on Robotics and Automation*, 2007, pp. 2004–2009.

[8] A. Leone, C. Distante, A. Mastrolia, and G. Indiverr, “A fully automated approach for underwater mosaicking,” in *MTS/IEEE OCEANS Conference*, Boston, USA, September 2006, pp. 1–6.

[9] O. Pizarro and H. Singh, “Toward large-area mosaicing for underwater scientific applications,” *IEEE Journal of Oceanic Engineering*, vol. 28, no. 4, pp. 651–672, October 2003.

[10] R. Garcia, J. Batlle, X. Cufí, and J. Amat, “Positioning an underwater vehicle through image mosaicking,” in *IEEE International Conference on Robotics and Automation*, vol. 3, Seoul, Rep. of Korea, May 2001, pp. 2779–2784.

[11] J. Ferrer, A. Elibol, O. Delaunoy, N. Gracias, and R. Garcia, “Large-area photo-mosaics using global alignment and navigation data,” in *MTS/IEEE OCEANS Conference*, Vancouver, Canada, November 2007, pp. 1–9.

[12] H. Sawhney, S. Hsu, and R. Kumar, “Robust video mosaicing through topology inference and local to global alignment,” in *European Conference on Computer Vision*, vol. II, Freiburg, Germany, June 1998, pp. 103–119.

[13] D. Gledhill, G. Tian, D. Taylor, and D. Clarke, “Panoramic imaging–a review,” *Computers & Graphics*, vol. 27, no. 3, pp. 435–445, 2003.

[14] V. Ila, J. M. Porta, and J. Andrade-Cetto, "Information-based compact pose SLAM," *Robotics, IEEE Transactions on*, vol. 26, no. 1, pp. 78–93, Feb. 2010.

[15] H. Bulow and A. Birk, "Fast and robust photomapping with an unmanned aerial vehicle UAV," in *IEEE/RSJ International Conference on Intelligent Robots and Systems, 2009. IROS 2009.*, 2009, pp. 3368–3373.

[16] F. Ferreira, G. Veruggio, M. Caccia, and G. Bruzzone, "Real-time optical SLAM-based mosaicking for unmanned underwater vehicles," *Intelligent Service Robotics*, vol. 5, pp. 55–71, 2012.

[17] D. Steedly, C. Pal, and R. Szeliski, "Efficiently registering video into panoramic mosaics," in *Tenth IEEE International Conference on Computer Vision, ICCV.*, vol. 2, 2005, pp. 1300–1307.

[18] M. Fadaeieslam, M. Fathy, and M. Soryani, "Key frames selection into panoramic mosaics," in *ICICS 2009. 7th International Conference on Information, Communications and Signal Processing*, dec. 2009, pp. 1–5.

[19] B. Zitová and J. Flusser, "Image registration methods: A survey," *Image and Vision Computing*, vol. 21, no. 11, pp. 977–1000, 2003.

[20] C. G. Harris and M. J. Stephens, "A combined corner and edge detector," in *Alvey Vision Conference*, Manchester, U.K., 1988, pp. 147–151.

[21] P. R. Beaudet, "Rotational invariant image operators," in *IAPR International Conference on Pattern Recognition*, 1978, pp. 579–583.

[22] T. Lindeberg, "Feature detection with automatic scale selection," *International Journal of Computer Vision*, vol. 30, no. 2, pp. 77–116, 1998.

[23] D. Lowe, "Distinctive image features from scale-invariant keypoints," *International Journal of Computer Vision*, vol. 60, no. 2, pp. 91–110, 2004.

[24] H. Bay, T. Tuytelaars, and L. Van Gool, "SURF: Speeded up robust features," in *European Conference on Computer Vision*, Graz, Austria, May 2006, pp. 404–417.

[25] K. Mikolajczyk and C. Schmid, "A performance evaluation of local descriptors," *IEEE Transactions on Pattern Analysis and Machine Intelligence*, vol. 27, no. 10, pp. 1615–1630, 2005.

[26] R. Hartley and A. Zisserman, *Multiple View Geometry in Computer Vision*, 2nd ed. Harlow, UK: Cambridge University Press, 2004.

[27] B. Triggs, P. McLauchlan, R. Hartley, and A. Fitzgibbon, "Bundle adjustment – A modern synthesis," in *Vision Algorithms: Theory and Practice*, ser. LNCS. Springer Verlag, 2000, pp. 298–375.

[28] O. Mason and M. Verwoerd, "Graph theory and networks in biology," *IET Systems Biology*, vol. 1, no. 2, pp. 89 –119, march 2007.

[29] N. Deo, *Graph theory with applications to engineering and computer science*. PHI Learning Pvt. Ltd., 2004.

[30] J. Gross and J. Yellen, *Graph theory and its applications*. Chapman & Hall/CRC, 2005.

[31] S. Skiena, *Implementing Discrete Mathematics: Combinatorics and Graph Theory with Mathematica*. Reading, MA: Addison-Wesley, 1990.

[32] T. Kavitha, C. Liebchen, K. Mehlhorn, D. Michail, R. Rizzi, T. Ueckerdt, and K. A. Zweig, "Cycle bases in graphs characterization, algorithms, complexity, and applications," *Computer Science Review*, vol. 3, no. 4, pp. 199–243, 2009.

[33] A. Elibol, N. Gracias, and R. Garcia, *Efficient Topology Estimation for Large Scale Optical Mapping*, ser. Springer Tracts in Advanced Robotics. Springer, 2012, vol. 82.

[34] B. Grocholsky, "Information-theoretic control of multiple sensor platforms," Ph.D. dissertation, University of Sydney, 2002.

[35] B. D. O. Anderson and J. B. Moore, *Optimal filtering*. Prentice-Hall, 1979.

[36] R. Prados, R. Garcia, N. Gracias, J. Escartin, and L. Neumann, "A novel blending technique for underwater gigamosaicing," *IEEE Journal of Oceanic Engineering*, vol. 37, no. 4, pp. 626–644, October 2012.